



**HAL**  
open science

## Coherent thermal transport in nano-phononic crystals: An overview

Zhongwei Zhang, Yangyu Guo, Marc Bescond, Jie Chen, Masahiro Nomura,  
Sebastian Volz

► **To cite this version:**

Zhongwei Zhang, Yangyu Guo, Marc Bescond, Jie Chen, Masahiro Nomura, et al.. Coherent thermal transport in nano-phononic crystals: An overview. *APL Materials*, 2021, 9, 10.1063/5.0059024 . hal-03420116

**HAL Id: hal-03420116**

**<https://hal.science/hal-03420116v1>**

Submitted on 9 Nov 2021

**HAL** is a multi-disciplinary open access archive for the deposit and dissemination of scientific research documents, whether they are published or not. The documents may come from teaching and research institutions in France or abroad, or from public or private research centers.

L'archive ouverte pluridisciplinaire **HAL**, est destinée au dépôt et à la diffusion de documents scientifiques de niveau recherche, publiés ou non, émanant des établissements d'enseignement et de recherche français ou étrangers, des laboratoires publics ou privés.

See discussions, stats, and author profiles for this publication at: <https://www.researchgate.net/publication/353648756>

# Coherent thermal transport in nano-phononic crystals: An overview

Article in *APL Materials* · August 2021

DOI: 10.1063/5.0059024

CITATIONS

0

READS

126

6 authors, including:



**Zhongwei Zhang**

The University of Tokyo

61 PUBLICATIONS 974 CITATIONS

[SEE PROFILE](#)



**Yangyu Guo**

Claude Bernard University Lyon 1

46 PUBLICATIONS 515 CITATIONS

[SEE PROFILE](#)



**Marc Bescond**

French National Centre for Scientific Research

140 PUBLICATIONS 1,308 CITATIONS

[SEE PROFILE](#)



**Jie Chen**

Tongji University

70 PUBLICATIONS 2,624 CITATIONS

[SEE PROFILE](#)

Some of the authors of this publication are also working on these related projects:



Nanowire Transistors [View project](#)



Thermoelectric properties of nanostructures [View project](#)

# Coherent thermal transport in nano-phononic crystals: An overview

Cite as: APL Mater. 9, 081102 (2021); doi: 10.1063/5.0059024

Submitted: 4 June 2021 • Accepted: 21 July 2021 •

Published Online: 2 August 2021



View Online



Export Citation



CrossMark

Zhongwei Zhang,<sup>1,a)</sup>  Yangyu Guo,<sup>1</sup>  Marc Bescond,<sup>2</sup> Jie Chen,<sup>3,4</sup>  Masahiro Nomura,<sup>1,b)</sup>   
and Sebastian Volz<sup>1,2,4,c)</sup> 

## AFFILIATIONS

<sup>1</sup>Institute of Industrial Science, The University of Tokyo, Tokyo 153-8505, Japan

<sup>2</sup>Laboratory for Integrated Micro and Mechatronic Systems, CNRS-IIS UMI 2820, The University of Tokyo, Tokyo 153-8505, Japan

<sup>3</sup>Center for Phononics and Thermal Energy Science, School of Physics Science and Engineering, Tongji University, 200092 Shanghai, People's Republic of China

<sup>4</sup>China-EU Joint Lab for Nano-Phononics, Tongji University, 200092 Shanghai, People's Republic of China

**Note:** This paper is part of the Special Topic on Phononic Crystals at Various Frequencies.

<sup>a)</sup> **Author to whom correspondence should be addressed:** [zhongwei@iis.u-tokyo.ac.jp](mailto:zhongwei@iis.u-tokyo.ac.jp)

<sup>b)</sup> **Electronic mail:** [nomura@iis.u-tokyo.ac.jp](mailto:nomura@iis.u-tokyo.ac.jp)

<sup>c)</sup> **Electronic mail:** [volz@iis.u-tokyo.ac.jp](mailto:volz@iis.u-tokyo.ac.jp)

## ABSTRACT

Nano-phononic crystals have attracted a great deal of research interest in the field of nanoscale thermal transport due to their unique coherent thermal transport behavior. So far, there have been many advances in the theory and simulation studies of coherent thermal transport in nano-phononic crystals. In this paper, we summarize the state-of-the-art studies in this field from the perspective of coherent thermal transport at low temperatures, minimum thermal conductivity, Anderson localization, in various nanosystems, and in the frame of machine learning driven studies. Each part is specifically presented under different simulation methodologies, in which the background theories are also summarized. Accordingly, the controversies between different methodologies in describing wave-like/coherent and particle-like/incoherent thermal phonons are discussed. Various effects on coherent thermal transport are reviewed, including interface roughness, mass disorder, structural randomness, aperiodic ordering, and temperature effect. Finally, an outlook on the future research on coherent thermal transport in nano-phononic crystals is given. This overview provides fundamental and advanced knowledge to understand the coherent thermal transport in nano-phononic crystals, which will be beneficial to the further understanding of the physical picture of thermal phonons and heat transfer related applications.

© 2021 Author(s). All article content, except where otherwise noted, is licensed under a Creative Commons Attribution (CC BY) license (<http://creativecommons.org/licenses/by/4.0/>). <https://doi.org/10.1063/5.0059024>

## I. INTRODUCTION

Phononic crystals are artificial materials designed to control the propagation properties of sound or elastic waves by introducing a secondary periodicity.<sup>1–3</sup> Within the new periodicity induced by the phononic crystals, the wave-related or coherent behavior of phonons is modified by the interference between the lattice waves, assuming the phase conservation of phonon waves during their dynamics and propagation. In the recent decades, miniaturization of devices and higher power density of electronics have made thermal conduction and management in nanostructures one of the most important research directions.<sup>4–10</sup> On the other hand, the downsizing of

phononic crystals to the nanoscale has given rise to the nanostructuring of nano-phononic crystals. Nano-phononic crystals are first studied in the context of solid one-dimensional layered materials known as superlattices<sup>11</sup> and generalized to nanomaterials with two-dimensional (2D) and three-dimensional (3D) periodicities. Generally speaking, when the characteristic size, i.e., period length, is comparable to the wavelength/mean free path (MFP)/coherence length of phonons responsible for thermal transport<sup>12–16</sup> (see the schematic figure in Fig. 1), which is typically in the range of 1–100 nm, a nanoscale phononic crystal provides a new opportunity to engineer thermal properties of materials using the wave nature of phonons. Different from bulk or microscale materials, the novel wave-related

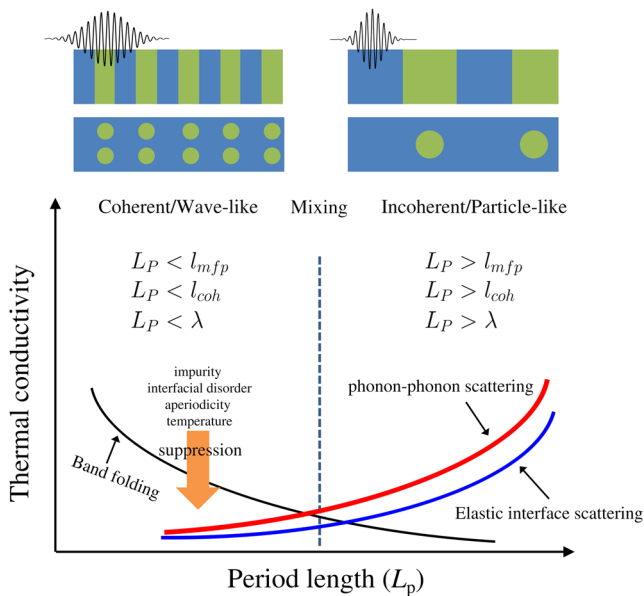


**FIG. 1.** Schematic of thermal transport in nano-phononic crystals. Thermal transport can be divided into coherent, incoherent, and their mixing transports. The transport regimes are determined by the comparison between period length ( $L_p$ ) and phonon mean free path ( $l_{mfp}$ )/coherence length ( $l_{coh}$ )/wavelength ( $\lambda$ ). The dependence of thermal conductivity on period length is correlated with different phonon scattering processes.

phonon physics and thermal transport properties make coherent thermal transport in nano-phononic crystals a hot research topic in the field of nanoscale thermal transport, which receives considerable attention.

So far, various coherent thermal transport phenomena in nano-phononic crystals have been reported. In summary, there are two contrasting pictures to describe phononic thermal transport: the particle-like/incoherent phonons and the wave-like/coherent phonons. The experimental study of the coherent thermal phonons is still challenging, as few experimental measurements are reported,<sup>13,17–20</sup> while the findings from theoretical and simulation works based on various atomistic approaches and theories have shown that the coherent thermal transport in nano-phononic crystals can be classified into three regimes (see Fig. 1): (1) coherence dominated, (2) incoherence dominated, and (3) mixed coherent and incoherent.<sup>12,14,17,21,22</sup> In general, certain approaches can only be used to study thermal transport in a given regime. For example, the coherent phonon-dominated regime at a short period length and at low temperatures is always studied when targeting the phonon dispersion modification from the secondary periodicity.<sup>22–27</sup> By treating the secondary periodicity as the origin of diffuse scattering, the Boltzmann transport equation (BTE) and Monte Carlo (MC) simulation with bulk modes are applied to study the incoherent thermal transport,<sup>28–30</sup> while non-equilibrium Green's function (NEGF)<sup>31–34</sup> and molecular dynamics (MD) simulation are performed to investigate the mixed regime.<sup>14,21,35–37</sup> Many influencing factors on the coherent thermal transport in nano-phononic crystals are reported by these methods, such as the atomic disorder at

the interface, structural randomness, disordered period, and temperature effect.<sup>14,21,22,30,35–39</sup> These coherent effects show that engineering coherent phonons is a promising way to tune the thermal conductivity in nano-phononic crystals. Moreover, with the rapid development of computer science, the combination of coherent thermal transport and machine learning has yielded advances in recent years by various groups.<sup>40–44</sup>

On the other hand, the diversely used methods also highlight the complexity and controversial viewpoints in the study and understanding of coherent thermal transport in nano-phononic crystals. For example, although the modified phonon dispersion from secondary periodicity is applied, the BTE calculations may not be able to fully account for the effect of phonon coherence on thermal transport since they only considering the particle nature of phonons.<sup>45–47</sup> The studies also show that MD simulation is a promising method that can simultaneously capture the wave- and particle-like pictures of thermal phonons, for instance, the minimum thermal conductivity and Anderson localization in Si/Ge superlattice and graphene-based porous nano-phononic crystals.<sup>14,48–52</sup> However, theory is still lacking to understand and uncover the “entangled” incoherent and coherent thermal transports in nano-phononic crystals from a modal level. How and where the coherence of thermal phonons transitions with period length in nano-phononic crystals is still a subject of research. Moreover, the factors influencing the coherent thermal transport, as explored by various methods, are quite massive and complex. In short, a further review or summary of the coherent thermal transport in nano-phononic crystals is needed from the perspective of theory and simulation studies, and possible solutions to controversies or debates.

From a material perspective, the coherent thermal transport is found in both composite nano-phononic crystals and unitary nano-phononic crystals. Composite nano-phononic crystals are mostly the combination of binary materials that have close lattice constants, for instance, Si/Ge,<sup>23,48,53–55</sup> GaAs/AlAs,<sup>17</sup> SrTiO<sub>3</sub>/CaTiO<sub>3</sub>,<sup>13</sup> graphene/hexagonal boron nitride superlattices,<sup>14,36,56</sup> or interfaces of nanoparticle embedded crystals.<sup>57,58</sup> Regarding unitary nano-phononic crystals, porous silicon is the most studied system,<sup>16,19,22,59</sup> and others are emerging in the field of two-dimensional materials, such as porous graphene nano-phononic crystals<sup>52,60</sup> and the isotopic or holey graphene/pristine graphene superlattices.<sup>37,50,61</sup> Some pillar-based materials, especially in the silicon system, are also proposed to study coherent phonon hybridization.<sup>62–64</sup> The majority of the nano-phononic crystals are initially designed for thermoelectric applications with significantly suppressed thermal conductivity in the incoherent region.<sup>65–67</sup> The explored high thermal conductivity due to constructive interference,<sup>13,17</sup> as well as low thermal conductivity due to destructive interference in the coherent regime (i.e., Anderson localization),<sup>19,68,69</sup> can also provide promising avenues for thermal transport engineering from the wave-like picture of thermal phonons.

In this paper, we provide a review on the up-to-date understanding of coherent thermal transport in nano-phononic crystals from the perspective of theoretical and simulation studies. The rest of this paper is organized as follows: In Sec. II, we first summarize coherent thermal transport at low temperatures and outline the importance of dispersion modification at low frequencies. In Sec. III, we review the studies on the minimum thermal conductivity from different approaches, including BTE, atomistic NEGF, and

MD simulations. Then, we summarize a specific phonon wave transport phenomenon, i.e., Anderson localization, from various reports in Sec. IV. In Sec. V, we present other unique coherent thermal transports, such as resonant thermal transport, two-path phonon interference. We have also summarized the advanced studies on the combination of machine learning and coherent thermal transport in Sec. VI. Finally, we present a brief outlook and conclusion for this review.

## II. COHERENT THERMAL TRANSPORT AT LOW TEMPERATURES

Due to the band-folding effect, nano-phononic crystals with a short period length can be treated as a homogeneous material for the coherent modes throughout the folded Brillouin zone.<sup>12,18</sup> However, the roughness, interfaces, or intrinsic phonon scattering usually partially destroy their coherence when they propagate over

multiple periods, and their transport becomes incoherent.<sup>39,70</sup> It is interesting to note that the phase-destroying processes for phonons always start from the high frequencies, as they are often involved in the diffuse scattering processes.<sup>52,71,72</sup> This mechanism leads to the fact that the higher frequency phonons cannot maintain their coherence even if some of them have a large wavelength in the secondary periodicity, while the lower frequency phonons dominate the coherent thermal transport when excited at low temperatures. Moreover, as the periodicity increases, a significant modulation of the band folding is observed for low-frequency modes, as indicated by the shift in the bandgap to the lower frequency region [see Figs. 2(a)–2(c)].<sup>22</sup> Recently, the study of coherent thermal transport at low temperatures, focusing exclusively on the low-frequency coherent phonons, has drawn increasing interest. The modulation of the Brillouin zone band folding on the group velocity and phonon density of states dominates the thermal transport in this regime.<sup>3,22,23,25–27,53,73–77</sup>

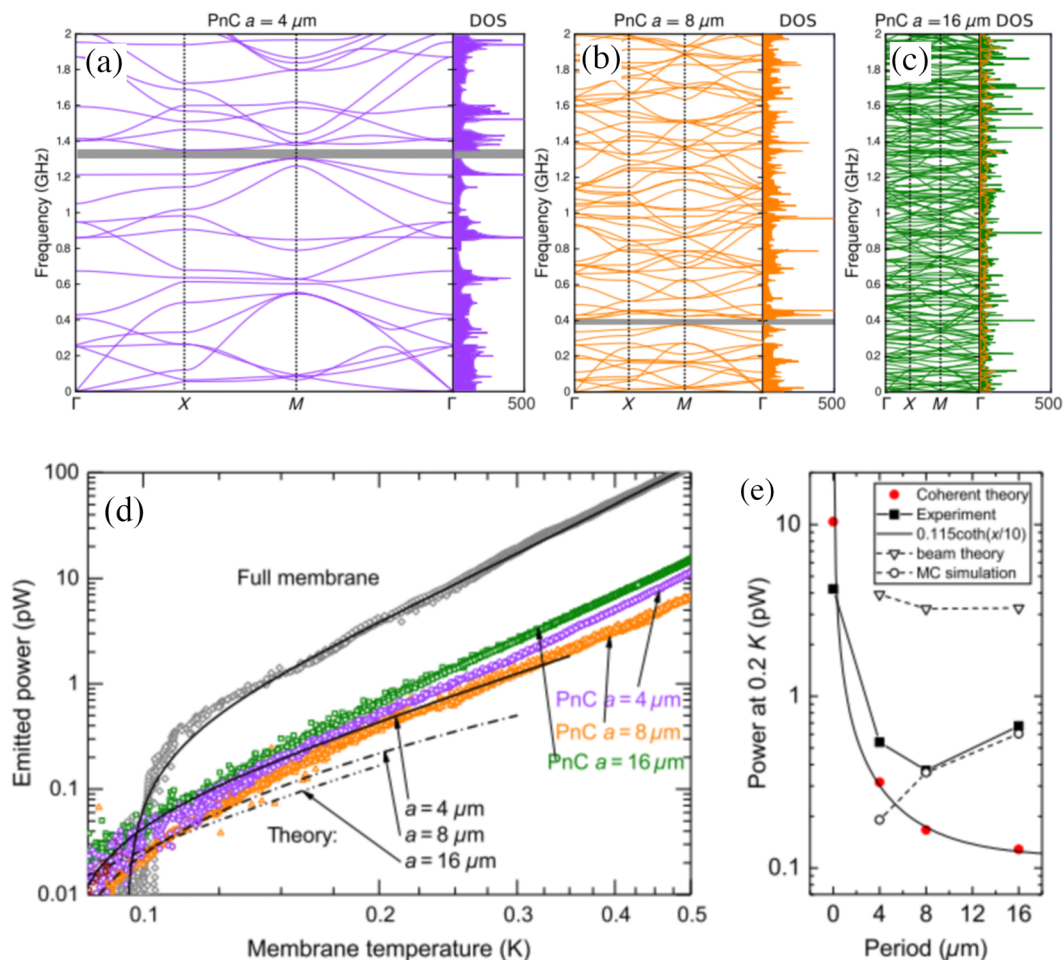


**FIG. 2.** Coherent thermal transport at low temperatures. [(a)–(c)] Phonon dispersion of a SiN membrane phononic crystal with different period lengths. (d) Emitted power of the SiN membrane and phononic crystal with different period lengths vs membrane temperature. (e) Emitted power of a SiN phononic crystal from different simulations vs period length. Reprinted figures with permission from Tian *et al.*, Phys. Rev. Appl. **12**, 014008 (2019). Copyright 2019 American Physical Society.

Hylgaard and Mahan<sup>53</sup> and Tamura *et al.*<sup>23</sup> predicted that due to the flattening of the dispersion curves resulting from the Brillouin zone folding, the phonon group velocity and also the ratio of thermal conductivity to phonon relaxation time in the Si/Ge superlattice are reduced by an order of magnitude. These studies took into account the changes in phonon group velocity and density of states and, in this way, purely estimated the coherence effect on thermal transport due to the phononic structures. Regarding practical devices, these studies should be valid only at low temperatures, such as sub-kelvins and mimikelvins. By implementing other methods, low-temperature coherent phenomena are also demonstrated.<sup>3,22,25–27,73–77</sup>

To estimate the coherent thermal transport in a silicon nitride (SiN) phononic crystal, Zen *et al.*<sup>3,22,25</sup> proposed to calculate the ballistic phonon emission. The radiated power is defined as

$$P(T) = \frac{1}{(2\pi)^2} \sum_j \oint_\gamma d\gamma \int_{\mathbf{k}} d\mathbf{k} \hbar \omega_j(\mathbf{k}) n(\omega_j, T) \times \frac{\partial \omega_j(\mathbf{k})}{\partial \mathbf{k}} \cdot \hat{\mathbf{n}}_\gamma \Theta \left( \frac{\partial \omega_j}{\partial \mathbf{k}} \cdot \hat{\mathbf{n}}_\gamma \right), \quad (1)$$

where  $\omega_j(\mathbf{k})$  refers to the mode frequency and  $n(\omega_j, T)$  is the Bose–Einstein distribution.  $\gamma$  is the heater-element boundary, and the contribution from modes with group velocities  $\partial \omega_j(\mathbf{k})/\partial \mathbf{k}$  projected on the normal to the heater boundary surface  $\hat{\mathbf{n}}_\gamma$  is taken into account by a step function  $\Theta$ . The emitted power in Figs. 2(d) and 2(e) indicates that at a sub-kelvin temperature, the coherent thermal transport can be gradually suppressed by increasing the periodicities. The calculated results in Fig. 2(d) agree well with the experimental measurements at a short period. This reduction in coherent thermal transport due to periodicities or period size is also found in the porous Si nano-phononic crystal.<sup>26,74</sup> Moreover, this coherent transport is strongly temperature dependent but relies less on the lattice type and the transverse dimension.

Note that these studies depended on the density of states and phonon group velocity only consider the purely coherent effect.<sup>3,22,25–27,73–77</sup> When continuously increasing the period or temperature, the coherent effect should be gradually weakened, and the incoherent/particle-like behavior of phonons becomes important, as shown in Fig. 2(e), indicating invalidity to fully capture the physical picture of phonons at larger period lengths. Moreover, because of the large size of phononic crystals, the phonon properties are always calculated by using the elastodynamic wave equation in the frequency region below a few tens of GHz. However, the phonons in the high-frequency region that might dominate the diffuse interface scattering or surface scattering can not be adequately considered.<sup>71,72,78,79</sup> The atomic disorder, impurity, and surface defects, which can dephase the phonon waves,<sup>37,52,80–83</sup> are all neglected. The atomistic methodologies should be applied further at relatively high temperature.

At low temperatures, especially in the range of sub-kelvins, the phonon–phonon scattering that can dephase the elastic waves becomes negligible, and the wavelength of the dominant thermal phonons is increased by more than two orders of magnitude, indicating the much longer propagating length of coherent phonons. Therefore, the thermal transport in this coherent region is mostly ballistic. The relationship between thermal conductivity ( $\kappa$ ) and thermal conductance ( $\sigma$ ) writes  $\kappa = \sigma L$ , where  $L$  is the length of the

system. In the purely coherent regime, since the thermal conductance remains constant, the thermal conductivity should be divergent with the length of nano-phononic crystals.<sup>8,84,85</sup> Moreover, the effects of phonon dephasing, such as interface atom or mass disorder and temperature, on thermal transport can be also estimated from the size dependence.

By applying the atomistic NEGF, the linear length dependent thermal conductivity was first reported in the AlAs/GaAs superlattice [see Figs. 3(a) and 3(b)], evidencing the pure ballistic thermal transport in this coherent regime.<sup>17</sup> In addition, the interface roughness can greatly affect the transmission of high-frequency phonons, but less low-frequency phonons. Obviously, the increase in interface roughness can suppress the coherent thermal transport by enhancing the diffuse interfacial scattering,<sup>17,38,73,86,87</sup> which further weakens the length dependence of thermal transport in Figs. 3(a) and 3(c). As temperature increases, a larger range of high-frequency modes are excited and incoherent phonon transport plays an increasing role. Accordingly, the length dependence of thermal conductivity is weakened due to the incoherent propagation of newly excited high-frequency phonons,<sup>73</sup> as shown in Fig. 3(d) for the case of the Si/Ge superlattice.

Overall, the coherent transport is mainly dominated by low-frequency phonons with long wavelengths, making their coherent behaviors easily observable at low temperatures. However, these low-temperature studies neglected some other sufficient dephasing processes, for instance, the diffuse scattering involving high-frequency phonons in the elastodynamic wave equation and phonon–phonon scattering in NEGF. As the system shifts from the purely coherent regime, like by continuously increasing the period length of the nano-phononic crystal or temperature, the enhanced diffuse scatterings can lead to a raise in incoherent phonons. Eventually, other intriguing thermal transport phenomena appear, such as minimum thermal conductivity, as summarized in Sec. III.

### III. MINIMUM THERMAL CONDUCTIVITY

After the minimum thermal conductivity was experimentally observed in the GaAs/AlAs superlattice<sup>88</sup> and Bi<sub>2</sub>Te<sub>3</sub>/Sb<sub>2</sub>Te<sub>3</sub> superlattice,<sup>89</sup> in which the cross-plane thermal conductivity recovers in the short period limit, many theoretical models and simulation methods have been developed to understand the coherent thermal transport in nano-phononic crystals.<sup>21,53,90–92</sup> However, the regime around the transition, i.e., the point of minimum thermal conductivity, from the incoherent to the coherent is due to the mixing of phononic and bulk modes and diverse scattering processes. There is still debate about the exact mechanisms involved, but much progress has been made in recent decades. In this section, we summarize the progress from theory and simulations on the study of minimum thermal conductivity in nano-phononic crystals. To emphasize the different mechanisms in thermal transport, the studies are specifically classified under different methodologies in which different mechanisms are considered.

#### A. Boltzmann transport equation

##### 1. Simkin–Mahan model

The BTE is one of the prevailing methods widely used in the study of thermal conductivity by incorporating various scatterings,

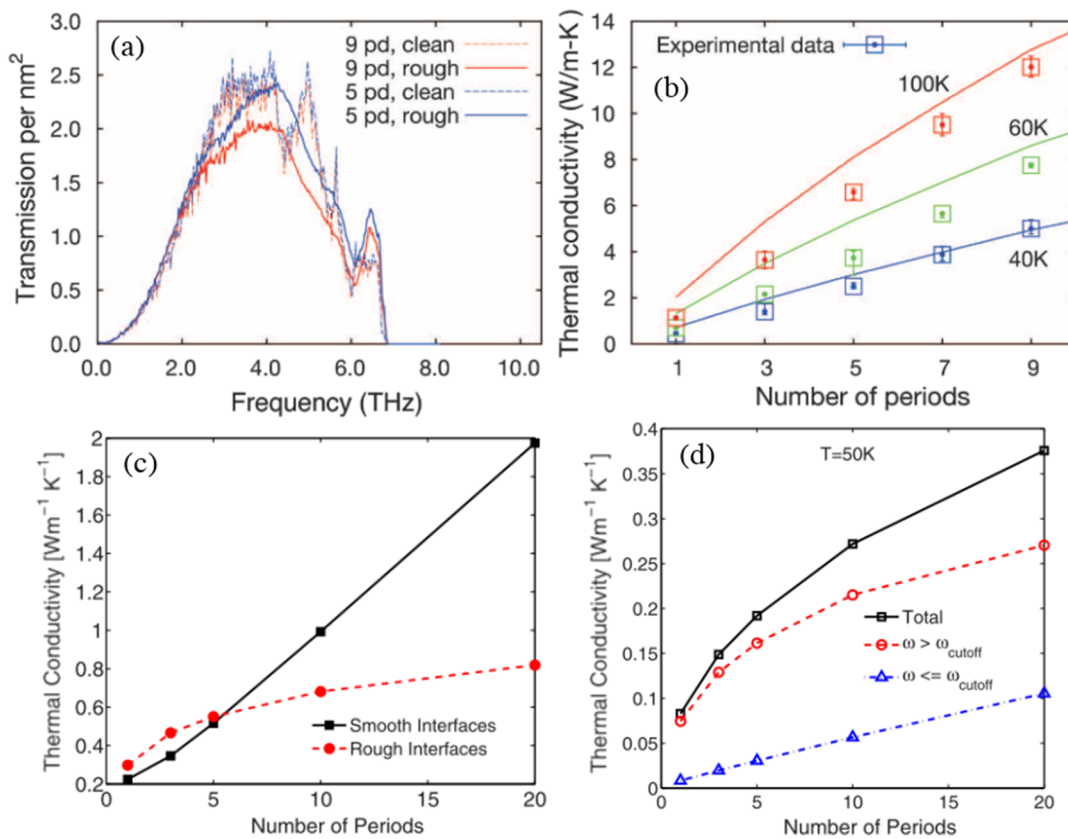


**FIG. 3.** Coherent thermal transport at low temperatures. (a) Transmission function with different period lengths of AlAs/GaAs superlattices with clean and rough interfaces. (b) Thermal conductivity of AlAs/GaAs superlattices vs period number at different temperatures. The dots are experimental measurements. Figures (a) and (b) reprinted with permission from Luckyanova *et al.*, Science **338**, 936 (2012). Copyright 2012 AAAS. (c) Length dependent thermal conductivity of Si/Ge superlattices with clean and rough interfaces. (d) Length dependent thermal conductivities of Si/Ge superlattices from different frequency regions at a rough interface. The frequency regions are classified by the frequency of the lowest acoustic phonon branch at the zone edge. Reprinted figures (c) and (d) with permission from Z. Tian, K. Esfarjani, and G. Chen, Phys. Rev. B **89**, 235307 (2014). Copyright 2014 American Physical Society.

such as phonon–phonon scattering, diffuse interface scattering and impurity scattering.<sup>4,46,93–95</sup> The initial study of thermal conductivity reduction in nano-phononic crystals begins with phononic crystals having large period lengths, where the particle picture prevails and is properly described by the BTE theory. Because the wave features of phonons are not considered in the BTE, this latter equation fails to explain the thermal conductivity increase in the short period limit and, thus, the minimum thermal conductivity. To fully cover the phonon behaviors with the BTE theory, both wave- and particle-like behaviors, Simkin and Mahan<sup>90</sup> innovatively proposed the following equation:

$$\kappa(T) = k_B l_{mfp} \sum_j \int \frac{d^d k}{(2\pi)^d} |v_z(\mathbf{k})|, \quad (2)$$

where  $j$  denotes the band index and  $l_{mfp}$  refers to the modal independent MFP. The wave theory yields the actual group velocity  $v_z(\mathbf{k})$  of the superlattice along the transport  $z$  direction. This formula is used to calculate the thermal conductivity from the usual formula in  $d$  dimensions. The MFP of nano-phononic crystals is widely used to

determine the transport regime of thermal phonons. When the layer thickness exceeds the MFP, then interference effects should diminish, and the particle model should become applicable. Reversely, the wave model should apply. Simkin and Mahan<sup>90</sup> proposed a phenomenological method to include this MFP  $l_{mfp}$  effect by adding an imaginary part  $i/l_{mfp}$  to the wave vector  $\mathbf{k}$ . This model was originally proposed by Prutton<sup>96</sup> for the electron energy band.

This model has been demonstrated applicable to phonon transport in the partially coherent regime, where bulk and superlattice phonon modes mix up. The calculated thermal conductivity for an artificial three-dimensional nano-phononic crystal is reported in Fig. 4(a). The system with a longer MFP exhibits more distinguishable coherent phonons, which can propagate through the interfaces as a wave before decay. Correspondingly, the position of the minimum thermal conductivity is also MFP dependent. The longer the MFP, the longer the period length for the minimum position, indicating a stronger coherent thermal transport. In this study, the other scatterings that can dephase the phonon waves are not separately included, and the MFP can be considered as

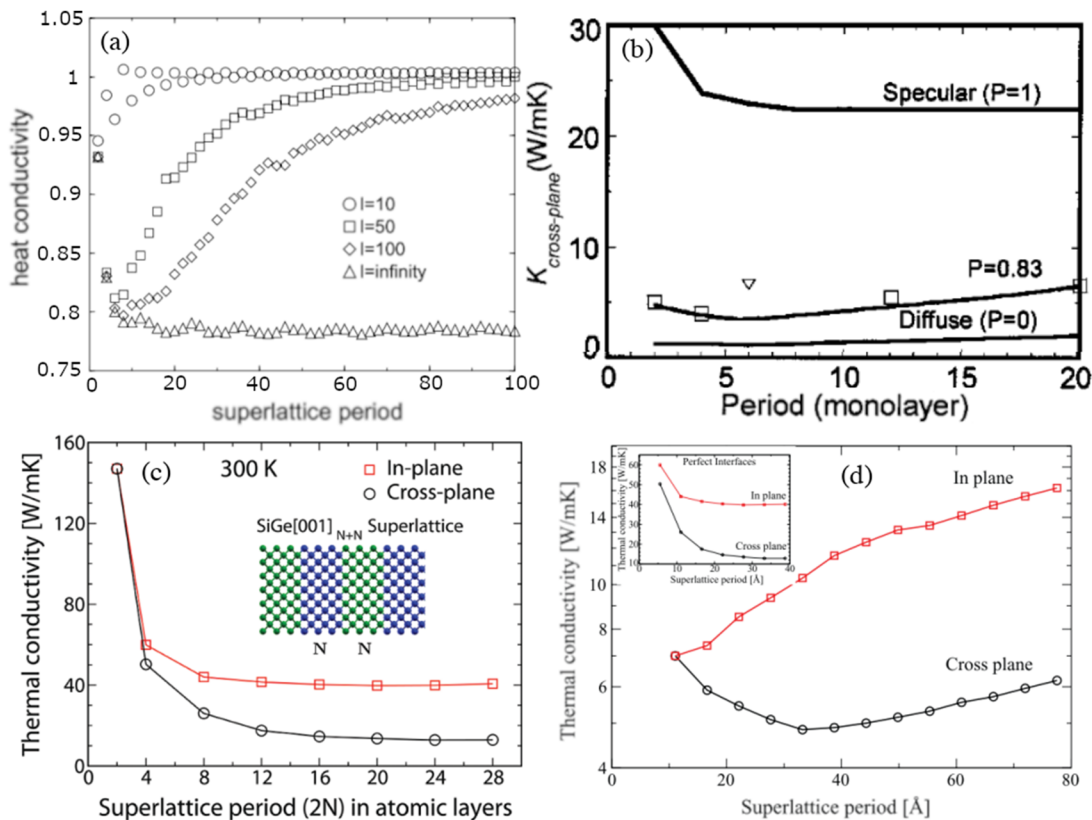


**FIG. 4.** Coherent thermal transport studies based on the Boltzmann transport equation. (a) Heat conductivity of three-dimensional superlattices vs period length with different mean free paths ( $l$ ). Reprinted figure (a) with permission from M. V. Simkin and G. D. Mahan, Phys. Rev. Lett. **84**, 927 (2000). Copyright 2000 American Physical Society. (b) Thermal conductivity of the GaAs/AlAs superlattice vs period length with different interface roughness. Reprinted figure (b) with permission from B. Yang and G. Chen, Phys. Rev. B **67**, 195311 (2003). Copyright 2003 American Physical Society. (c) Thermal conductivity of ideal Si/Ge superlattices with perfect interfaces vs period length. Reprinted figure (c) with permission from J. Garg, N. Bonini, and N. Marzari, Nano Lett. **11**, 5135 (2011). Copyright 2011 American Chemical Society. (d) Thermal conductivity of Si/Ge superlattices with different interface roughness vs period length. Reprinted figure (d) with permission from J. Garg and G. Chen, Phys. Rev. B **87**, 140302 (2013). Copyright 2013 American Physical Society.

gathering all the scattering processes that define the propagation length.

With the same model, a further study showed that the detailed interface scattering process in GaAs/AlAs superlattices can significantly affect the coherent transport and the minimum thermal conductivity [see Fig. 4(b)].<sup>91</sup> In nano-phononic crystals that have a smooth interface with specular scattering, the system exhibits strong coherent transport behavior. Increasing the roughness of the interface makes the interface scattering reach a diffusive limit, and the coherent transport gradually disappears. Obviously, the interface scattering can significantly destruct the interference of phonon waves. Nevertheless, the Simkin–Mahan model cannot quantitatively estimate the thermal conductivity values.

## 2. Density functional theory based studies

With the development of computer science, more accurate approaches are proposed to describe the various properties in condensed matter physics, such as the density functional theory (DFT).<sup>97–102</sup> A first-principles-based BTE approach

using the harmonic and anharmonic force constants derived from DFT has been gradually developed for studying thermal conductivity<sup>94,103–105,177</sup>

On the basis of DFT and BTE calculations, Garg *et al.*<sup>29</sup> found that the thermal conductivity of ideal Si/Ge superlattices, with perfect interfaces, does not display any minimum [see Fig. 4(c)], but the calculated values first decrease and then converge to a constant value at a large period length. This trend is consistent with previous lattice dynamics calculations,<sup>3,22,25–27,73–77</sup> in which the pure coherent/wave-like behaviors from band folding are considered. However, this trend does not agree with the experimental results<sup>13,18,88,89</sup> and also with most studies using the Simkin–Mahan model,<sup>90,91</sup> in which even the specular interface also yields the minimum thermal conductivity. The converged trend in the large period indicates that the dephasing processes in the system are insufficient to generate particle-like phonons. It should be noted that the virtual crystal method<sup>106,107</sup> was applied to calculate the phonon dispersion of nano-phononic crystals due to the large size of the unit cell. The effect of the interface on phonon dispersion has been

included; however, the interface scattering has been underestimated. As further studied by Garg and Chen,<sup>92</sup> the minimum thermal conductivity can appear again as further including the interfacial disorder scattering term [see Fig. 4(d)]. This fully recovering of the observed minimum thermal conductivity indicates that the realistic transport phenomenon is a mixed process combining at least three effects, i.e., group velocity reduction and density of states change from band folding, interfacial disorder, and finally intrinsic anharmonic phonon–phonon scattering. An alternative method to compute the phonon dispersion of nano-phononic crystals is expected to develop and explore, especially in taking into account the simultaneous bulk and phononic modes around the minimum thermal conductivity.

Besides the minimum thermal conductivity, the BTE is also applied to understand the reduced thermal conductivity in nano-phononic crystals. The decrease in thermal conductivity with decreasing period size is always understood as an incoherent phonon boundary scattering effect. However, the BTE modeling cannot fully recover the trend, and its predictions are always larger than the experimental values.<sup>12,59,108,109</sup> Those latter studies found that a partial coherent treatment of phonons can improve the modeling results, where phonons are regarded as either wave or particles depending on their frequency dependent MFPs.<sup>12</sup> Phonons with an MFP smaller than the characteristic size of phononic crystals are treated as particles, and the transport in this regime is modeled by the BTE with phonon boundary scattering taken into account. On the other hand, phonons with an MFP longer than the

characteristic size are treated as waves. In this regime, the phonon dispersion relations should be modified according to the secondary periodicity, in which the zone folding effect is exactly included. By this way, Dechaumphai and Chen<sup>12</sup> accurately predicted the thermal transport in the incoherence dominated regime in nano-phononic crystals.

## B. Atomistic non-equilibrium Green's function

Previously, the atomistic NEGF has been demonstrated as an efficient approach to study the interfacial thermal transport.<sup>31,78,110</sup> Different from the BTE calculations, the NEGF usually does not consider the anharmonic phonon–phonon scatterings. Although several advances in the anharmonic NEGF have been proposed,<sup>34,111,112</sup> the NEGF study of thermal transport in nano-phononic crystals still focuses on the ballistic region due to the huge computational cost, as we summarized in Sec. II. We emphasize that atomistic NEGF calculations natively describe the wave nature of thermal phonons by solving the atomic dynamic equation.<sup>34,111,112</sup>

Through NEGF calculations, the minimum thermal conductance is found in the isotopic graphene superlattice<sup>35</sup> and graphene/hBN superlattice<sup>36</sup> [see Figs. 5(a) and 5(b)], even with a perfect interface. The increase in thermal conductance in the large period evidences the weakened suppression of thermal transport, resulting from the weakened diffuse elastic scatterings at interfaces and the released localization modes at interfaces.<sup>36</sup> Obviously, in these studies, the phonon–phonon scattering, which is the main

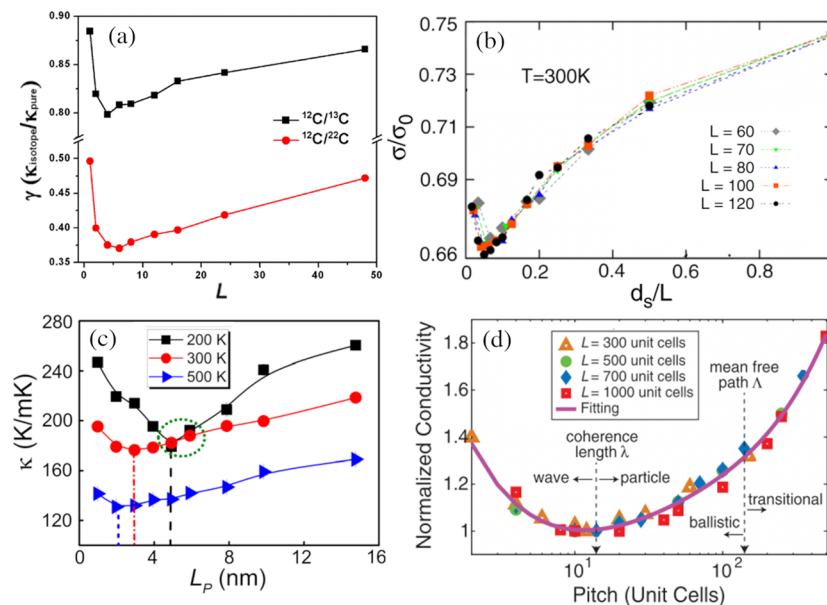


**FIG. 5.** Coherent thermal transport studies based on non-equilibrium Green's function and molecular dynamics simulations. (a) Thermal conductivity of isotopic graphene superlattice vs period length. Figure (a) is reprinted with permission from Ouyang *et al.*, *Europhys. Lett.* **88**, 028002 (2009). Copyright 2009 EPL Association. (b) Thermal conductivity of the graphene/hBN superlattice vs period length with different total lengths. Reprinted with permission from J.-W. Jiang, J.-S. Wang, and B.-S. Wang, *Appl. Phys. Lett.* **99**, 043109 (2011). Copyright 2011 AIP Publishing LLC. Figures (a) and (b) are obtained from non-equilibrium Green's function calculations. (c) Thermal conductivity of graphene/hBN superlattices vs period length at different temperatures. Reprinted with permission from Chen *et al.*, *Appl. Phys. Lett.* **109**, 023101 (2016). Copyright 2016 AIP Publishing LLC. (d) Normalized thermal conductivity of graphene/hBN superlattices vs period length with different fixed total lengths. Reprinted figure (d) with permission from T. Zhu and E. Ertekin, *Phys. Rev. B* **90**, 195209 (2014). Copyright 2014 American Physical Society. Figures (a) and (b) are obtained from the molecular dynamics simulations.

process destroying the phase of phonon waves, does not exist. The minimum thermal conductivity in NEGF calculations should be directly related to the roughness degree of interfaces. As the interfaces are too smooth to prevent the interfacial diffuse elastic scattering, there should be no minimum thermal conductivity due to the too weak incoherent transport at large periods.<sup>29,92</sup> For the two-dimensional nano-phononic crystals, although without the interfacial disorder, the relatively large atomic lattice spacing is likely to impede the phase of phonon waves. This might be the reason why the minimum thermal conductivity was never reported in the three-dimensional material based phononic crystals when having perfect interfaces, such as Si/Ge superlattices.<sup>29,73,92</sup> Further studies and comparisons are still expected to clarify this dimensionality or lattice spacing effect on coherence suppression through interfaces in nano-phononic crystals.

Interestingly, the minimum thermal conductances always appear at a constant ratio of period length ( $d_s$ ) and system length ( $L$ ),  $\sim d_s/L = 0.05\%$  [see Fig. 5(b)].<sup>36</sup> In the ballistic regime, because of the limited diffuse interface scattering and absence of phonon–phonon scatterings, the MFP ( $l_{mfp}$ ) can be considered as linearly dependent on the system length  $L$ , i.e.,  $l_{mfp} \sim L$ . Therefore, the period size where the minimum thermal conductivity emerges should be less length dependent at high temperatures as the MFP has been largely suppressed by the phonon–phonon scatterings. This trend has been observed in other studies using MD simulations as we discuss in Sec. III C. Therefore, the NEGF is powerful in simulating the coherent thermal transport by including a broad range of phonon scattering processes, while the effect of temperature excited phonon–phonon scatterings on coherence could not be explored, so far.

### C. Molecular dynamic simulations

The atomistic MD simulations can provide a classical description of the dynamic evolution of atomic systems.<sup>7,113–115</sup> The coherent/wave nature of thermal phonons can be natively captured by those simulations in the atomic motions. Volz *et al.*<sup>114</sup> found that the thermal conductivity of Si/Ge superlattices can be computed from MD simulations, and the values agree well with the results from BTE calculations based on the phonon particle model. While this study was mainly focusing on the superlattices with relatively large period lengths, the coherent regime was not explored.

Later, the coherent thermal transport and minimum thermal conductivity have been found through MD simulations in GaAl/GaAs superlattices,<sup>116,117</sup> Si/Ge superlattices,<sup>48,118</sup> and also other two-dimensional nano-phononic crystals,<sup>14,37,50–52,56,61,119</sup> especially graphene-based nano-phononic crystals. Similar to the findings from other methodologies summarized before, those studies mostly demonstrated that the interface roughness, surface mismatch, or structural randomness can significantly suppress the coherent thermal conductivity and even dismiss the minimum thermal conductivity phenomenon. On the other hand, the significant temperature effect on minimum thermal conductivity was also reported [see Fig. 5(c)], in which the minimum shifts to a shorter period length with the increase in temperature,<sup>51,52</sup> due to the raising impact of phonon–phonon scatterings on dephasing. There are also other influencing factors on thermal transport, for instance, the strain effect through the thermo–mechanical correlation.<sup>120</sup> By

softening the phonon branches and correspondingly decreasing the group velocity, the strain can result in the reduction of coherent thermal transport in the superlattice.<sup>61</sup> However, in terms of coherence qualities, such as temporal coherence time or spatial coherence length, more research is expected.

Interestingly, a length independent minimum thermal conductivity was reported. Zhu and Ertekin<sup>14</sup> found that the minimum thermal conductivity is independent of the total length of a graphene/hBN superlattice, and the minimum always appears at the period length around 4–8 nm at room temperature [see Fig. 5(d)]. Moreover, this directly corresponds to the coherence length of the superlattice. The calculation of phonon coherence length in this work is extended from the blackbody radiation,<sup>28,121,122</sup> while its validation and physical figure for thermal phonons should be further verified. The length independent trend is also reported by Hu and Poulikakos<sup>48</sup> in Si/Ge nanowires. Moreover, although including different intrinsic phonon properties, the minimum thermal conductivities in graphene/hBN superlattices and Si/Ge nanowires mostly appear in similar period lengths.<sup>14,48,123,124</sup> This might be the reason why the overall coherence length in nano-phononic crystals has been significantly suppressed to an ultra-low value, by the interface scattering and phonon–phonon scatterings at elevated temperatures. Actually, further analysis and comparison on coherence length estimation in different dimensional nano-phononic crystals are expected.

The MD simulations can also provide the modal-level information from the normal mode decomposition method<sup>125–128</sup> to provide insight into the modal dependent coherence of thermal phonons. Some interesting phenomena related to the coherent thermal transport are reported. With the transmission decomposition method, Hu *et al.*<sup>52</sup> found that, in porous graphene nano-phononic crystals, the transmission of high-frequency phonons can be suppressed by the aperiodicity, while the low-frequency phonons with a long wavelength can maintain the transmission efficiency. The results qualitatively agree with the NEGF calculations. In addition, with the normal mode decomposition method, Da Silvia *et al.*<sup>56</sup> found that the phonon lifetimes do not obviously change with period length, and the minimum thermal conductivity is just a result of the band-folding effect, which is somehow controversial to the reduction in diffuse interface scattering at a large period length. Moreover, the observed temperature effect<sup>51,52</sup> also indicates the non-negligible role of phonon lifetime on coherent thermal transport.

On one side, the normal mode decomposition of MD trajectory greatly depends on the projection basis defined by the primitive cell of the nanostructures. For large periods, the bulk modes are predominant. However, in the binary composites (such as ABABAB. . .), the primitive cells are not identical (A or B). Then, on switching to smaller periods, the phonon modes of the secondary periodicity are excited, and the unit cell (AB) of nano-phononic crystals should be treated as the primitive cell. However, the transition is unclear and should be modal dependent, as the low-frequency phonons are more coherent than those of high frequencies. On the other side, considering that only the particle behavior is included in the normal mode decomposition method,<sup>129–131</sup> the phonon lifetimes obtained from this method might be invalid anymore in the coherence dominated regime.

In addition, the coherent behavior of thermal phonons in nano-phononic crystals has also been the object of other MD simulations.

Chen *et al.*<sup>118</sup> found that the coherent thermal transport can be explained by the superposition of vibrational density of states of Si and Ge in Si/Ge superlattices, indicating that the wave effect in the coherent regime modifies the phonon properties. Moreover, the folded bands can also be observed in the density of states as resonance frequency peaks.<sup>51</sup> The minimum thermal conductivity in nano-phononic crystals also provides an opportunity for optimizing thermoelectrics. MD simulation has been widely used in the pursuit of further suppressing minimum thermal conductivity, for instance, by combining machine learning, as we summarized in Sec. VI.

#### D. Decomposition into coherent and incoherent phonon conductions

As discussed above, the coherent thermal transport in nano-phononic crystals can be modeled by different simulation approaches. However, even in the coherence dominated regime, the thermal conductivity always combined different phonon contributions,<sup>13,124,132,133</sup> i.e., coherent and incoherent. How to distinguish or decompose the thermal conductivity into this dual picture? The decomposition would be meaningful for the understanding of the coherent thermal transport, the wave nature of phonons, and also the generation of coherent phonons in nano-phononic crystals.

The main approach consists in separately treating the incoherent and coherent contributions with different methodologies. In the incoherent regime, the pure particle based theories apply. For example, the BTE<sup>12</sup> and MC simulation<sup>66,134</sup> are applied to study the pure incoherent propagation, in which the effect of phononic structure is included by considering the boundary scattering effects. On the other hand, the coherent thermal conductivity is studied by considering the band-folding effect in nano-phononic crystals, in which the new phonon dispersion of the nano-phononic crystal is taken into account.<sup>12,66,134</sup> Those studies also found that the criterion to distinguish coherent and incoherent phonons should operate at the modal level. As implemented by Dechaumphai and Chen,<sup>12</sup> if the MFP is larger than the characteristic size for a specific mode, the incoherent theory is implemented and reversely the coherent one is used. In a few works, the total thermal conductivity is understood as the simple superposition of separately calculated incoherent and coherent thermal conductivities.<sup>66</sup> After these treatments, the agreement between the calculated thermal conductivity and experimental results can be improved in some degree [see Fig. 6(a)]. However, these approaches cannot provide more insight into the nature of coherent phonons and their propagation. Moreover, the distinction between the modal-level coherent and incoherent phonons is still under debate as the wave-like behavior of phonons is more related to coherent length/time rather than the widely used MFP (see Fig. 1).<sup>124,133</sup>

On the other hand, the coherent and incoherent thermal transports can be simultaneously captured in MD simulations. In this scheme, researchers decompose the total thermal conductivity into coherent and incoherent components. Based on the MD simulations in conceptual binary Lennard-Jones systems, Wang *et al.*<sup>132</sup> proposed a two-phonon model that divides the overall heat conduction into coherent and incoherent phonon contributions. The length dependent thermal conductance of periodic nano-phononic crystals  $G_{PC}(L)$  can be expressed as

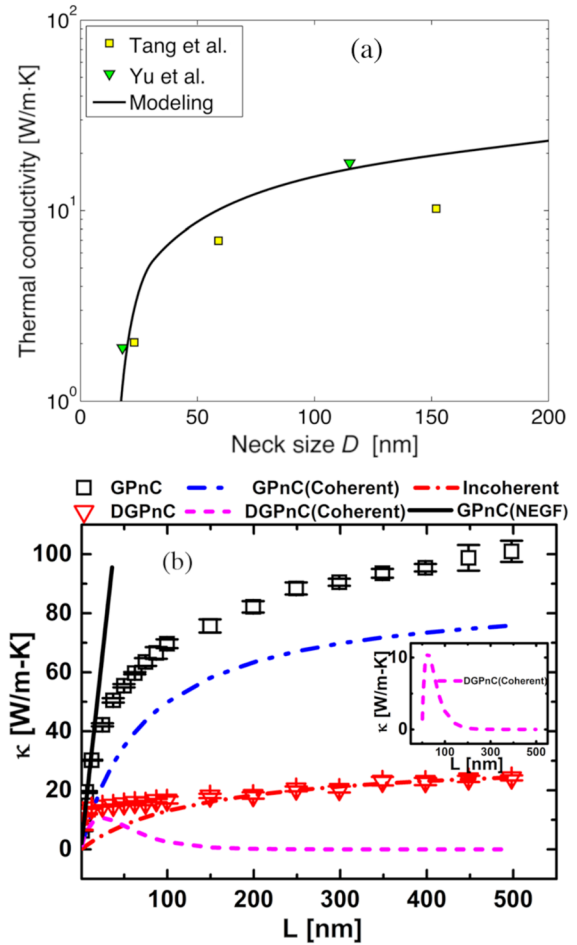


**FIG. 6.** Decomposition into coherent and incoherent phonon conductions. (a) Modeled room-temperature thermal conductivity of Si phononic crystals as a function of neck size (solid line), compared with the experimental data in Refs. 59 and 109 (symbols), in which the coherent and incoherent thermal transports are separately treated. Reprinted with permission from E. Dechaumphai and R. Chen, *J. Appl. Phys.* 111, 073508 (2012). Copyright 2012 AIP Publishing LLC. (b) Decomposed coherent and incoherent thermal conductivities in graphene nano-phononic crystals (GPnC) and disordered graphene nano-phononic crystals (DGPnC). The inset of (b) reports the purely coherent contribution. Reprinted figure (b) with permission from Hu *et al.*, *J. Phys. Chem. Lett.* 9, 3959 (2018). Copyright 2018 American Physical Society.

$$G_{PC}(L) = G_{PC,coh}(L) + G_{inc}(L) = G_{coh,0}(L) \frac{l_{coh}}{l_{coh} + L} + G_{inc,0}(L) \frac{l_{inc}}{l_{inc} + L}, \quad (3)$$

where the subscript 0 indicates the ballistic-limit quantity. The length dependence is derived from the Landauer framework.<sup>135</sup>  $l_{coh}$  and  $l_{inc}$  are the respective MFPs of the coherent phonons and incoherent phonons. If the disorder is introduced into the nano-phononic crystals, the Anderson localization of coherent phonons would lead to the exponential decay of thermal conductance when  $L$  increases (see the detailed discussion about the Anderson

localization in Sec. IV). Then, the thermal conductance of disordered nano-phononic crystals  $G_{\text{DPC}}(L)$  can be rewritten as

$$G_{\text{DPC}}(L) = G_{\text{DPC,coh}}(L) + G_{\text{inc}}(L) \\ = G_{\text{coh},0}(L) \frac{l_{\text{coh}}}{l_{\text{coh}} + L} e^{-\frac{L}{l_{\text{loc}}}} + G_{\text{inc},0}(L) \frac{l_{\text{inc}}}{l_{\text{inc}} + L}, \quad (4)$$

where  $l_{\text{loc}}$  is the localization length, which describes how fast  $G$  decays in random media. When  $L$  is large, the coherent thermal transport becomes negligible as it decays much faster compared to the incoherent term. Thus, at large  $L$  values,  $G_{\text{inc}}$  can be obtained. When the size is reduced,  $G_{\text{coh}}$  contributed by coherent phonons may be significant, which can be obtained by subtracting  $G_{\text{DPC}}(L)$  from  $G_{\text{PC}}(L)$ . With this two-phonon model, Wang *et al.*<sup>132</sup> found that coherent phonons dominate the thermal transport of ordered nano-phononic crystals over a large length scale, while this contribution can be exponentially decayed in disordered nano-phononic crystals. The same tendency was also reported in graphene porous nano-phononic crystals with this dual-phonon model by Hu *et al.*

[see Fig. 6(b)].<sup>52</sup> Moreover, they also demonstrated that (1) coherent phonons with a long MFP increase the thermal conductivity with  $L$  indicating the ballistic transport behavior; (2) coherent phonons can be easily localized by the structural disorder or randomness.<sup>37,52,132</sup> As we can see, several quantities need to be fitted as a function of  $L$ , which might induce uncertainties in the model. The gray approximation or the independence to frequency used here cannot reveal more insights. The above summaries indicate that the coherence of thermal phonons should be modal or wavelength dependent, a further decomposition at the modal level is highly expected to understand the coherent thermal and transition between transports.

#### IV. ANDERSON LOCALIZATION

Localization is a well-known wave phenomenon that significantly impedes transport, as uncovered by a pioneering work of Anderson.<sup>136</sup> The localization of thermal phonons as another engineering based on the wave nature of phonons is widely represented

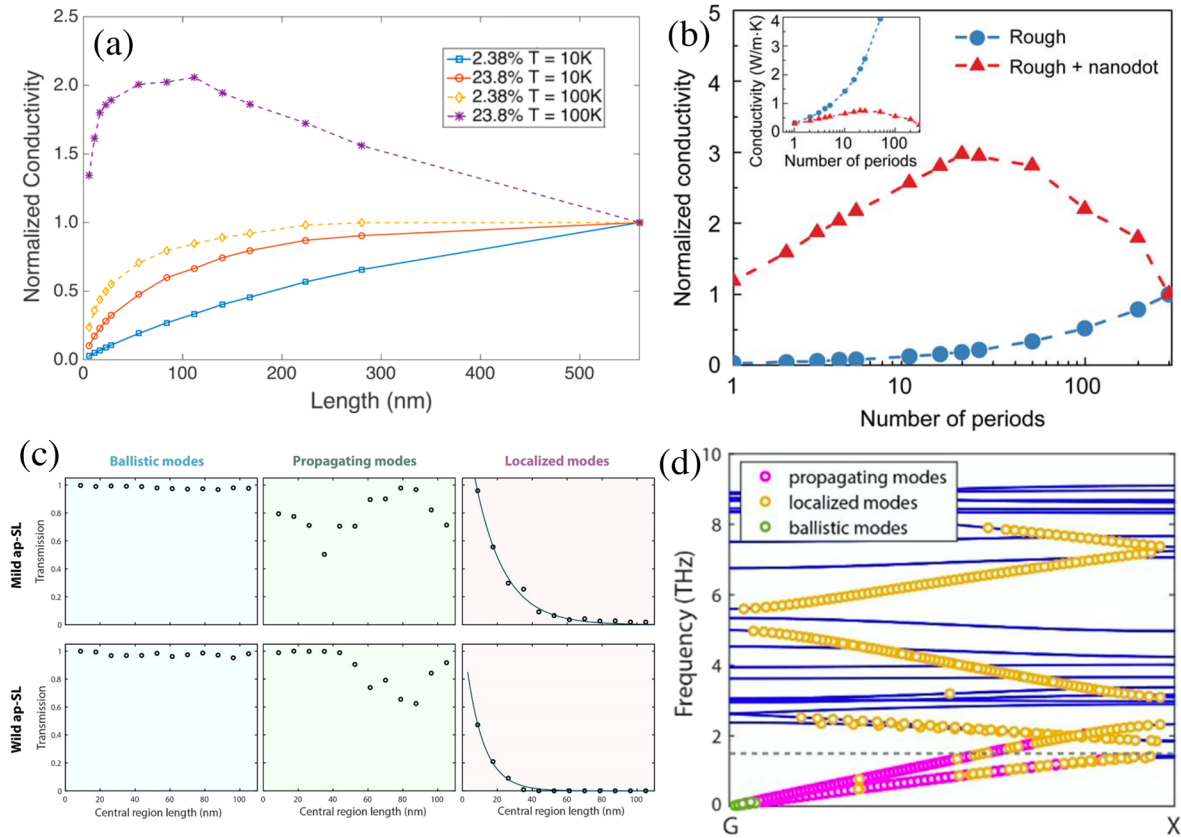


**FIG. 7.** Anderson localization of coherent thermal phonons in nano-phononic crystals. (a) Normalized thermal conductivity vs length of GaAs/AlAs superlattices with 2.38% and 23.8% ErAs interfacial coverage at  $T = 10$  and  $T = 100$  K. Anderson localization leads to the local thermal conductivity maximum. Reprinted figure (a) with permission from J. Mendoza and G. Chen, *Nano Lett.* **16**, 7616 (2016). Copyright 2016 American Physical Society. (b) Normalized thermal conductivity as a function of number of periods for a rough superlattice with and without ErAs nanodots at the interfaces at 30 K (inset shows thermal conductivity values). Figure (b) is reprinted with permission from Luckyanova *et al.*, *Sci. Adv.* **4**, eaat9460 (2018). Copyright 2018 AAAS. (c) The typical transmission patterns of ballistic mode, propagating mode, and localized mode in mild and wild aperiodic superlattices. (d) Projected modes in wild aperiodic superlattices to the phonon dispersion of periodic superlattices along gamma (G) to X. Reprinted figures (c) and (d) with permission from R. Hu and Z. Tian, *Phys. Rev. B* **103**, 045304 (2021). Copyright 2021 American Physical Society.

in disordered nano-phononic crystals.<sup>69</sup> The wave-related characteristic scales, i.e., wavelength or coherence length, mostly belong to the nanoscale, making the phonon localization in nano-phononic crystals extensively explored by atomistic simulation methods via either NEGF or MD simulations. The Anderson localization of thermal phonons is always studied from two aspects in disordered phononic crystals: (1) a maximum thermal conductivity with lengths and (2) an exponential decay of specific modal transmission with lengths. In this section, we summarize the recent progress in the study of phonon localization, specifically in the disordered nano-phononic crystals.

By randomly introducing ErAs particles in GaAs superlattices, through NEGF calculations, Mendoza and Chen<sup>38</sup> found a local thermal conductivity maximum as a function of length. Moreover, on increasing the temperature and disorder degree, the maximum thermal conductivity disappeared [see Fig. 7(a)]. Those dependences indicate that Anderson localization happens at relatively high frequency requiring thermal energy to increase phonon population and also high disorder in the system. Their further study<sup>68</sup> verified this point, even with a rough interface between GaAs and AlAs, but without ErAs particles, the Anderson localization cannot be observed, indicating it as a strong wave localization phenomenon [see Fig. 7(b)]. On the other hand, the studies of Anderson localization also evidenced that the wave behavior of thermal phonons is strongly mode dependent.<sup>38,39,68</sup> For example, ballistic modes, propagating modes, and localized modes are simultaneously observed in the same structure of Si/Ge aperiodic superlattices.<sup>39</sup> As shown in Fig. 7(c), the transmission of ballistic modes is fully length independent and that of propagating modes is also less dependent on length, while the localized modes fully decay to zero following an exponential law. Figure 7(d) further shows that the predominant phonons are from the acoustic branches in the low-frequency region, while localized phonon modes approximately correspond to the acoustic branches at the folded Brillouin zone boundary. It seems that Anderson localization is related to the wavelength of thermal phonons. As the wavelength approaches the size of the unit cell of phononic crystals that corresponds to the zone boundary of the folded Brillouin zone, phonons can be easily localized. The phonon wave features of the folded modes with different wavelengths and also their relationship to Anderson localization is still unclear and worth to be further explored. Moreover, the distinct localization phenomena of modes indicate that the Anderson localization should be studied from the modal level, and the thermal conductivity maximum contributed by the overall modal localization can only be reached in strongly disordered nano-phononic crystals when a wider range of modes is localized. The design of unique nano-phononic crystals with enhanced Anderson localization, making the localization measurable in experiments, still attracts lots of research interest.<sup>38,43,70,137</sup>

On the other hand, a partial localization phenomenon has also been found in MD simulations but rarely reported in NEGF studies. Compared to the full Anderson localization in which phonon transmission can entirely decay to zero following the exponential trend, the partial localization makes the transmission decay to a constant value with the system length.<sup>52,70,137</sup> The partial localization might be originated from the fact that anharmonicity can destroy the coherence of phonons, hence, canceling the Anderson localization, especially at relatively high frequency. In addition, the

disorder degree should be another effect that can tune the localization degree in aperiodic nano-phononic crystals. The Anderson localization has also been demonstrated to optimize the thermoelectrics as both minority charge carriers and phonons can be simultaneously localized.<sup>69</sup>

## V. HYBRIDIZATION AND TWO-PATH INTERFERENCES

The wave nature of thermal phonons is also responsible for other interesting wave-related phenomena in periodic nanostructures, such as resonance modes<sup>62–64,77,138–146</sup> and two-path phonon interference phenomena.<sup>57,58,147,148</sup> These can also engineer thermal transport based on the wave picture of thermal phonons. The phonon resonance was demonstrated by Chen *et al.*<sup>138</sup> in Si/Ge core-shell nanowires, in which phonon resonance corresponds to the localization of longitudinal modes that can further lead to the reduction in thermal conductivity. Later, phonon resonance has been extended to other nano-phononic crystals, and its effect on thermal transport is also extensively explored, for instance, in the case of pillar-based nano-phononic crystals.<sup>62,63,139,149</sup> It should be noted that pillar-based nanostructures are also demonstrated as the phononic metamaterials<sup>139</sup> as having the characteristics of a metamaterial.

The pillar-based resonant crystal was proposed by Davis and Hussein,<sup>62</sup> by erecting pillars on the surface of a silicon thin film without altering the base thin-film material. Due to the wave hybridization mechanism between the pillar local resonances and the base, the group velocity of the phonon spectrum as well as its thermal conductivity has been greatly suppressed [see Fig. 8(a)]. Thereafter, phonon resonance has been widely studied in pillar systems.<sup>63,64,77,139,140</sup> Those works have shown that thermal conductivity suppression is dominated by the reduction in group velocity, implying the wave hybridization effect on phonon dispersion. However, the decreasing lifetimes are also observed but limited around the resonance frequency region and in low magnitude.<sup>63</sup> This conclusion in some degree is different from the findings in the resonant host-guest systems, such as the clathrates, in which the phonon resonance modes not only suppress the group velocity due to the band crossing phenomena from the hybridization effect but also provides additional scattering channels for phonon-phonon scattering inside base crystals.<sup>142,143,145,146,150,151</sup> and some recent works in resonant Si nanowires.<sup>64,152</sup> In addition, the studies in pillar-based systems also demonstrated that the suppression effect from resonance modes on thermal conductivity reduces with size,<sup>63,77,139</sup> indicating the weakened wave resonance effect. Besides its effect on resonance frequency, the hybridization degree is another critical point, which also changes with the pillar size. However, a frame to understand the wave hybridization degree between local resonance and main base structures and the relationship of this hybridization degree to coherent thermal transport is still lacking.

Two-path phonon interference resonance is another intriguing method to engineer coherent thermal transport.<sup>57,58,147,153–155</sup> Kosevich *et al.*<sup>153</sup> found that the effects of phonon wave interference between different paths can be used for the control of heat transfer through interfaces and for the design of phonon metamirrors and meta-absorbers. Based on the two-path phonon interference, a phononic crystal nanocapacitor was proposed<sup>155</sup> for storage and lasing of coherent terahertz lattice waves. Recently, Hu *et al.*<sup>58</sup>

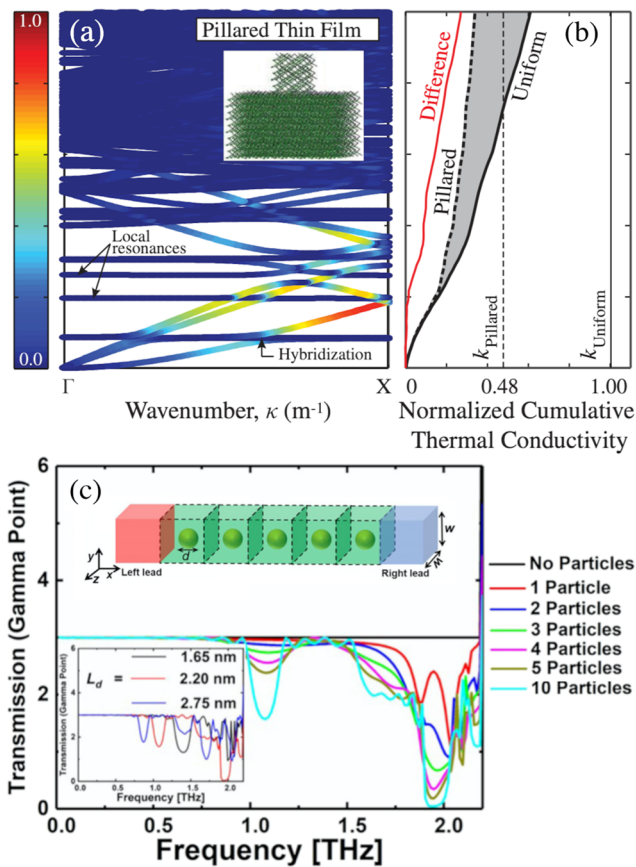


**FIG. 8.** Nano-phononic crystals realizing coherent thermal transport. A comparison of (a) the phonon dispersion and (b) the thermal conductivity of pillared silicon nano-phononic crystals. The dispersion curves are colored to represent the modal contribution to the cumulative thermal conductivity. Reprinted figures (a) and (b) with permission from B. L. Davis and M. I. Hussein, *Phys. Rev. Lett.* **112**, 055505 (2014). Copyright 2014 American Physical Society. (c) Low-frequency part of the phonon transmission spectrum for the two-path interference nano-phononic crystals. The insets show the schematic figure of the two-path interference system and the low-frequency part of the phonon transmission with different period distances  $L_d$ . Reprinted figures (c) with permission from Hu *et al.*, *Phys. Rev. B* **102**, 024301 (2020). Copyright 2020 American Physical Society.

found that two-path phonon interference resonance can induce a stop band in a special periodic crystal, in which a multilayer array of germanium nanoparticles is embedded in a crystalline silicon matrix [see Fig. 8(b)]. Due to this two-path phonon interference, a stop band with complete phonon reflection and a dramatic reduction in thermal conductance are found. Compared to the conventional nano-phononic crystals, coherent phonons are insensitive to the aperiodicity of two-path phonon interference.

## VI. MACHINE LEARNING-BASED STUDY

The minimum thermal conductivity of nano-phononic crystals provides a pathway for thermoelectric development, as we discussed in Sec. IV. Moreover, the studies also demonstrated that the minimum thermal conductivity can be further suppressed by

randomly re-arranging the periodicity,<sup>156</sup> i.e., using aperiodic phononic crystals. The suppression of thermal conductivity is mostly originated from the Anderson localization of coherent phonons. The thermal transport in phononic crystals significantly depends on the structural parameters, i.e., size of individual units,<sup>157</sup> mass and spatial ratio of units,<sup>40</sup> interfacial details,<sup>158</sup> which provides a very large design space to reach the lower limit of thermal conductivity. This represents a hard but attractive field to explore. On the other hand, materials informatics introduces a brand new way to accelerate the exploration of nano-phononic crystals with special properties.<sup>40,41,44,156,159–167</sup> A simple case is the application of machine learning-based potential to obtain the more accurate interatomic forces and energies than the ones emanating from empirical potentials for MD simulations.<sup>44,164,168</sup>

After the first introduction of the machine learning algorithms in the thermal transport field by Carrete *et al.*,<sup>159</sup> machine learning-based algorithms have been widely applied to study the thermal transport phononic crystals, which can sufficiently take into account different effects in nanostructures.<sup>40,41</sup> There are many studies focusing on the minimization of thermal conductivity in aperiodic nano-phononic crystals by maximizing the Anderson localization with different machine learning algorithms and thermal transport calculation methodologies. For example, by driving from the machine learning study, Roy Chowdhury *et al.*<sup>43</sup> found that the thermal conductivity in aperiodic phononic crystals can be further minimized 30% in comparison to the value of the minimum thermal conductivity in the periodic case. For more details about this field, please refer to other recent reviews.<sup>44,162,163,169</sup>

## VII. SUMMARY AND OUTLOOK

We present in this paper the state-of-the-art studies on the topics of coherent thermal transport in nano-phononic crystals from theory and simulation viewpoints. Diverse important coherent thermal transport behaviors are reviewed and discussed, including low-temperature coherent thermal transport, minimum thermal conductivity, Anderson localization, and coherent phonons in resonator and pillared nano-phononic crystals. The recent hot topic of machine learning driven coherent thermal transport is also introduced. Our review and discussions are conducted according to simulation methodologies. Considering that different methodologies capture distinct pictures of thermal phonons, i.e., wave- and particle-like, we try to clarify and summarize the controversies between methodologies, and also with experiments. For example, the studies of coherent thermal transport at low temperatures only consider the band-folding effect, i.e., purely coherent effects, while the minimum thermal conductivity can be found in the intermediate regime of coherent and incoherent thermal transport, in which the complexity makes it difficult to be adequately studied and understood. We have also reviewed the various influencing factors and effective pathways for engineering coherent thermal transport in nano-phononic crystals, such as interface roughness, mass disorder, structural randomness, aperiodic arrangement, and temperature effect. Correspondingly, several important behaviors and unique underlying physical mechanisms are presented for the understanding of coherent thermal phonons and their propagation. This paper provides a large set of information to understand and utilize coherent thermal transport.

The summarized coherent thermal transport not only brings a new opportunity to understand and engineer the nano-phononic crystals from a perspective view of wave/coherent picture of thermal phonons but also concludes several physical controversies in understanding and modeling coherent phonons. As we have discussed in Sec. II, the realistic coherent thermal transport in nano-phononic crystals is composed of different pictures. Usually, the BTE and NEGF calculations can partially simulate the influencing factors on coherent phonons. In BTE calculations, the treatment of the wave nature is only from the phonon dispersion change by considering the secondary periodicity, while the NEGF calculations usually do not consider phonon-phonon scatterings. A newly developed anharmonic NEGF methodology from our group<sup>34</sup> is expected to provide more insights into the coherent thermal transport in nano-phononic crystals by including more comprehensive scattering processes. Our review demonstrated that MD simulations might be a more powerful tool to study coherent phonons although ignoring the quantum effect, while a better modal-level decomposition approach is needed. The widely used normal mode decomposition from MD post-processing is still based on the particle-like nature of thermal phonons, somehow losing the wave description of phonons. Alternative approaches that can simultaneously capture wave- and particle-like pictures of thermal phonons are desired. Very recently, we proposed a generalized decay law for thermal phonons by including their intrinsic coherence.<sup>131</sup> We expect that this model can be applied to reveal the coherent nature of thermal phonons in nano-phononic crystals, especially for the problem of how thermal phonons transit from an incoherent to a coherent behavior with a period length at the modal level. Moreover, the explanations or descriptions of vibrational coherence in other fields are also expectedly applied to understand the coherence of thermal phonons, such as self-synchronization in optomechanical and biological systems.<sup>170–172</sup> On the other hand, recently, the wave-like/coherent behavior has also been defined in complex crystals or amorphous materials,<sup>173–176</sup> in which the overlap or superposition of phonon branches can result in an additional contribution to thermal conductivity. Physically, the relationship between those demonstrated coherent phonons and coherent phonons in nano-phononic crystals is appealing but still undisclosed. To conclude, we believe that the coherence of thermal phonons and also their propagation in nano-phononic crystals are still active research topics and worth attracting more interest in the future.

## ACKNOWLEDGMENTS

This work was supported by the CREST Japan Science and Technology Agency (Grant Nos. JPMJCR19I1 and JPMJCR19Q3).

## DATA AVAILABILITY

Data sharing is not applicable to this article as no new data were created or analyzed in this study.

## REFERENCES

- <sup>1</sup>S. Yang, J. H. Page, Z. Liu, M. L. Cowan, C. T. Chan, and P. Sheng, *Phys. Rev. Lett.* **93**, 024301 (2004).
- <sup>2</sup>A. Khelif and A. Adibi, *Phononic Crystals: Fundamentals and Applications* (Springer, Berlin, 2015), p. 23.
- <sup>3</sup>I. J. Maasilta, T. A. Puurtinen, Y. Tian, and Z. Geng, *J. Low Temp. Phys.* **184**, 211 (2016).
- <sup>4</sup>D. G. Cahill, W. K. Ford, K. E. Goodson, G. D. Mahan, A. Majumdar, H. J. Maris, R. Merlin, and S. R. Phillpot, *J. Appl. Phys.* **93**, 793 (2003).
- <sup>5</sup>T. Luo and G. Chen, *Phys. Chem. Chem. Phys.* **15**, 3389 (2013).
- <sup>6</sup>D. G. Cahill, P. V. Braun, G. Chen, D. R. Clarke, S. Fan, K. E. Goodson, P. Keblinski, W. P. King, G. D. Mahan, A. Majumdar, H. J. Maris, S. R. Phillpot, E. Pop, and L. Shi, *Appl. Phys. Rev.* **1**, 011305 (2014).
- <sup>7</sup>H. Bao, J. Chen, X. Gu, and B. Cao, *ES Energy Environ.* **1**, 16 (2018).
- <sup>8</sup>Z. Zhang, Y. Ouyang, Y. Cheng, J. Chen, N. Li, and G. Zhang, *Phys. Rep.* **860**, 1 (2020).
- <sup>9</sup>H. Wang, S. Hu, K. Takahashi, X. Zhang, H. Takamatsu, and J. Chen, *Nat. Commun.* **8**, 15843 (2017).
- <sup>10</sup>P. Jiang, S. Hu, Y. Ouyang, W. Ren, C. Yu, Z. Zhang, and J. Chen, *J. Appl. Phys.* **127**, 235101 (2020).
- <sup>11</sup>V. Narayanamurti, H. L. Störmer, M. A. Chin, A. C. Gossard, and W. Wiegmann, *Phys. Rev. Lett.* **43**, 2012 (1979).
- <sup>12</sup>E. Dechaumphai and R. Chen, *J. Appl. Phys.* **111**, 073508 (2012).
- <sup>13</sup>J. Ravichandran, A. K. Yadav, R. Cheaito, P. B. Rossen, A. Soukiasian, S. J. Suresha, J. C. Duda, B. M. Foley, C.-H. Lee, Y. Zhu, A. W. Lichtenberger, J. E. Moore, D. A. Muller, D. G. Schlom, P. E. Hopkins, A. Majumdar, R. Ramesh, and M. A. Zurbuchen, *Nat. Mater.* **13**, 168 (2014).
- <sup>14</sup>T. Zhu and E. Ertekin, *Phys. Rev. B* **90**, 195209 (2014).
- <sup>15</sup>G. Xie, D. Ding, and G. Zhang, *Adv. Phys.: X* **3**, 720 (2018).
- <sup>16</sup>M. Nomura, J. Shiomi, T. Shiga, and R. Anufriev, *Jpn. J. Appl. Phys., Part 1* **57**, 080101 (2018).
- <sup>17</sup>M. N. Luckyanova, J. Garg, K. Esfarjani, A. Jandl, M. T. Bulsara, A. J. Schmidt, A. J. Minnich, S. Chen, M. S. Dresselhaus, Z. Ren, E. A. Fitzgerald, and G. Chen, *Science* **338**, 936 (2012).
- <sup>18</sup>M. Maldovan, *Nat. Mater.* **14**, 667 (2015).
- <sup>19</sup>J. Maire, R. Anufriev, R. Yanagisawa, A. Ramiere, S. Volz, and M. Nomura, *Sci. Adv.* **3**, e1700027 (2017).
- <sup>20</sup>J. Lee, W. Lee, G. Wehmeyer, S. Dhuey, D. L. Olynick, S. Cabrini, C. Dames, J. J. Urban, and P. Yang, *Nat. Commun.* **8**, 14054 (2017).
- <sup>21</sup>Y. Chen, D. Li, J. R. Lukes, Z. Ni, and M. Chen, *Phys. Rev. B* **72**, 174302 (2005).
- <sup>22</sup>Y. Tian, T. A. Puurtinen, Z. Geng, and I. J. Maasilta, *Phys. Rev. Appl.* **12**, 014008 (2019); [arXiv:1904.09102](https://arxiv.org/abs/1904.09102).
- <sup>23</sup>S.-I. Tamura, Y. Tanaka, and H. J. Maris, *Phys. Rev. B* **60**, 2627 (1999).
- <sup>24</sup>W. E. Bies, R. J. Radtke, and H. Ehrenreich, *J. Appl. Phys.* **88**, 1498 (2000).
- <sup>25</sup>N. Zen, T. A. Puurtinen, T. J. Isotalo, S. Chaudhuri, and I. J. Maasilta, *Nat. Commun.* **5**, 3435 (2014).
- <sup>26</sup>R. Anufriev and M. Nomura, *Phys. Rev. B* **91**, 245417 (2015).
- <sup>27</sup>R. Anufriev, A. Ramiere, J. Maire, and M. Nomura, *Nat. Commun.* **8**, 15505 (2017).
- <sup>28</sup>G. Chen, *J. Heat Transfer* **119**, 220 (1997).
- <sup>29</sup>J. Garg, N. Bonini, and N. Marzari, *Nano Lett.* **11**, 5135 (2011).
- <sup>30</sup>A. Jain, Y.-J. Yu, and A. J. H. McGaughey, *Phys. Rev. B* **87**, 195301 (2013).
- <sup>31</sup>N. Mingo and L. Yang, *Phys. Rev. B* **68**, 245406 (2003).
- <sup>32</sup>N. Mingo, *Phys. Rev. B* **74**, 125402 (2006).
- <sup>33</sup>W. Zhang, T. S. Fisher, and N. Mingo, *J. Heat Transfer* **129**, 483 (2006).
- <sup>34</sup>Y. Guo, M. Bescond, Z. Zhang, M. Luisier, M. Nomura, and S. Volz, *Phys. Rev. B* **102**, 195412 (2020).
- <sup>35</sup>T. Ouyang, Y. P. Chen, K. K. Yang, and J. X. Zhong, *Europhys. Lett.* **88**, 028002 (2009).
- <sup>36</sup>J.-W. Jiang, J.-S. Wang, and B.-S. Wang, *Appl. Phys. Lett.* **99**, 043109 (2011).
- <sup>37</sup>S. Hu, Z. Zhang, P. Jiang, W. Ren, C. Yu, J. Shiomi, and J. Chen, *Nanoscale* **11**, 011839 (2019).
- <sup>38</sup>J. Mendoza and G. Chen, *Nano Lett.* **16**, 7616 (2016).
- <sup>39</sup>R. Hu and Z. Tian, *Phys. Rev. B* **103**, 045304 (2021).
- <sup>40</sup>S. Ju, T. Shiga, L. Feng, Z. Hou, K. Tsuda, and J. Shiomi, *Phys. Rev. X* **7**, 021024 (2017).
- <sup>41</sup>R. Hu, S. Iwamoto, L. Feng, S. Ju, S. Hu, M. Ohnishi, N. Nagai, K. Hirakawa, and J. Shiomi, *Phys. Rev. X* **10**, 021050 (2020).

- <sup>42</sup>P. Chakraborty, Y. Liu, T. Ma, X. Guo, L. Cao, R. Hu, and Y. Wang, *ACS Appl. Mater. Interfaces* **12**, 8795 (2020).
- <sup>43</sup>P. Roy Chowdhury, C. Reynolds, A. Garrett, T. Feng, S. P. Adiga, and X. Ruan, *Nano Energy* **69**, 104428 (2020).
- <sup>44</sup>Y. Ouyang, C. Yu, G. Yan, and J. Chen, *Front. Phys.* **16**, 43200 (2021).
- <sup>45</sup>R. Peierls, *Ann. Phys.* **395**, 1055 (1929).
- <sup>46</sup>M. Omini and A. Sparavigna, *Physica B* **212**, 101 (1995).
- <sup>47</sup>A. Cepellotti and N. Marzari, *Phys. Rev. X* **6**, 041013 (2016).
- <sup>48</sup>M. Hu and D. Poulikakos, *Nano Lett.* **12**, 5487 (2012).
- <sup>49</sup>K.-H. Lin and A. Strachan, *Phys. Rev. B* **87**, 115302 (2013).
- <sup>50</sup>X. Mu, T. Zhang, D. B. Go, and T. Luo, *Carbon* **83**, 208 (2015).
- <sup>51</sup>X.-K. Chen, Z.-X. Xie, W.-X. Zhou, L.-M. Tang, and K.-Q. Chen, *Appl. Phys. Lett.* **109**, 023101 (2016).
- <sup>52</sup>S. Hu, Z. Zhang, P. Jiang, J. Chen, S. Volz, M. Nomura, and B. Li, *J. Phys. Chem. Lett.* **9**, 3959 (2018).
- <sup>53</sup>P. Hyldgaard and G. D. Mahan, *Phys. Rev. B* **56**, 10754 (1997).
- <sup>54</sup>A. A. Kiselev, K. W. Kim, and M. A. Strosio, *Phys. Rev. B* **62**, 6896 (2000).
- <sup>55</sup>C. Dames and G. Chen, *J. Appl. Phys.* **95**, 682 (2004).
- <sup>56</sup>C. Da Silva, F. Saiz, D. A. Romero, and C. H. Amon, *Phys. Rev. B* **93**, 125427 (2016).
- <sup>57</sup>H. Han, L. G. Potyomina, A. A. Darinskii, S. Volz, and Y. A. Kosevich, *Phys. Rev. B* **89**, 180301 (2014).
- <sup>58</sup>S. Hu, L. Feng, C. Shao, I. A. Strelnikov, Y. A. Kosevich, and J. Shiomi, *Phys. Rev. B* **102**, 024301 (2020).
- <sup>59</sup>J. Tang, H.-T. Wang, D. H. Lee, M. Fardy, Z. Huo, T. P. Russell, and P. Yang, *Nano Lett.* **10**, 4279 (2010).
- <sup>60</sup>S. Hu, M. An, N. Yang, and B. Li, *Nanotechnology* **27**, 265702 (2016).
- <sup>61</sup>X. Wang, M. Wang, Y. Hong, Z. Wang, and J. Zhang, *Phys. Chem. Chem. Phys.* **19**, 24240 (2017).
- <sup>62</sup>B. L. Davis and M. I. Hussein, *Phys. Rev. Lett.* **112**, 055505 (2014).
- <sup>63</sup>H. Honarvar and M. I. Hussein, *Phys. Rev. B* **97**, 195413 (2018).
- <sup>64</sup>S. Xiong, K. Sääskilähti, Y. A. Kosevich, H. Han, D. Donadio, and S. Volz, *Phys. Rev. Lett.* **117**, 025503 (2016).
- <sup>65</sup>G. Xie, Z. Ju, K. Zhou, X. Wei, Z. Guo, Y. Cai, and G. Zhang, *npj Comput. Mater.* **4**, 21 (2018).
- <sup>66</sup>D. Ma, A. Arora, S. Deng, G. Xie, J. Shiomi, and N. Yang, *Mater. Today Phys.* **8**, 56 (2019).
- <sup>67</sup>K. Ren, X. Liu, S. Chen, Y. Cheng, W. Tang, and G. Zhang, *Adv. Funct. Mater.* **30**, 2004003 (2020).
- <sup>68</sup>M. N. Luckyanova, J. Mendoza, H. Lu, B. Song, S. Huang, J. Zhou, M. Li, Y. Dong, H. Zhou, J. Garlow, L. Wu, B. J. Kirby, A. J. Grutter, A. A. Puzos, Y. Zhu, M. S. Dresselhaus, A. Gossard, and G. Chen, *Sci. Adv.* **4**, eaat9460 (2018).
- <sup>69</sup>Z. Tian, *ACS Nano* **13**, 3750 (2019).
- <sup>70</sup>T. Juntunen, O. Vänskä, and I. Tittonen, *Phys. Rev. Lett.* **122**, 105901 (2019).
- <sup>71</sup>T. Feng, X. Ruan, Z. Ye, and B. Cao, *Phys. Rev. B* **91**, 224301 (2015).
- <sup>72</sup>S. Hu, J. Chen, N. Yang, and B. Li, *Carbon* **116**, 139 (2017).
- <sup>73</sup>Z. Tian, K. Esfarjani, and G. Chen, *Phys. Rev. B* **89**, 235307 (2014).
- <sup>74</sup>R. Anufriev and M. Nomura, *Phys. Rev. B* **93**, 045410 (2016).
- <sup>75</sup>T. Puurtinen and I. Maasilta, *Crystals* **6**, 72 (2016).
- <sup>76</sup>R. Anufriev, S. Gluchko, S. Volz, and M. Nomura, *ACS Nano* **12**, 011928 (2018).
- <sup>77</sup>R. Anufriev and M. Nomura, *Sci. Technol. Adv. Mater.* **19**, 863 (2018).
- <sup>78</sup>Z. Zhang, Y. Xie, Q. Peng, and Y. Chen, *Sci. Rep.* **6**, 21639 (2016).
- <sup>79</sup>Y. Guo, Z. Zhang, M. Bescond, S. Xiong, M. Nomura, and S. Volz, *Phys. Rev. B* **103**, 174306 (2021).
- <sup>80</sup>M. Hase, K. Ishioka, M. Kitajima, K. Ushida, and S. Hishita, *Appl. Phys. Lett.* **76**, 1258 (2000).
- <sup>81</sup>B. Krummheuer, V. M. Axt, T. Kuhn, I. D'Amico, and F. Rossi, *Phys. Rev. B* **71**, 235329 (2005).
- <sup>82</sup>M. Hase, Y. Miyamoto, and J. Tominaga, *Phys. Rev. B* **79**, 174112 (2009).
- <sup>83</sup>T. Jakubczyk, V. Delmonte, S. Fischbach, D. Wigger, D. E. Reiter, Q. Mermillod, P. Schnauber, A. Kaganskiy, J.-H. Schulze, A. Strittmatter, S. Rodt, W. Langbein, T. Kuhn, S. Reitzenstein, and J. Kasprzak, *ACS Photonics* **3**, 2461 (2016).
- <sup>84</sup>X. Gu, Y. Wei, X. Yin, B. Li, and R. Yang, *Rev. Mod. Phys.* **90**, 041002 (2018).
- <sup>85</sup>Z. Zhang and J. Chen, *Chin. Phys. B* **27**, 035101 (2018).
- <sup>86</sup>B. Qiu, G. Chen, and Z. Tian, *Nanoscale Microscale Thermophys. Eng.* **19**, 272 (2015).
- <sup>87</sup>Z. Tian, K. Esfarjani, and G. Chen, *Phys. Rev. B* **86**, 235304 (2012).
- <sup>88</sup>W. S. Capinski, H. J. Maris, T. Ruf, M. Cardona, K. Ploog, and D. S. Katzer, *Phys. Rev. B* **59**, 8105 (1999).
- <sup>89</sup>R. Venkatasubramanian, *Phys. Rev. B* **61**, 3091 (2000).
- <sup>90</sup>M. V. Simkin and G. D. Mahan, *Phys. Rev. Lett.* **84**, 927 (2000).
- <sup>91</sup>B. Yang and G. Chen, *Phys. Rev. B* **67**, 195311 (2003).
- <sup>92</sup>J. Garg and G. Chen, *Phys. Rev. B* **87**, 140302 (2013).
- <sup>93</sup>S. Pettersson, *J. Phys. C: Solid State Phys.* **20**, 1047 (1987).
- <sup>94</sup>L. Lindsay, *Nanoscale Microscale Thermophys. Eng.* **20**, 67 (2016).
- <sup>95</sup>Z. Zhang, Y. Xie, Y. Ouyang, and Y. Chen, *Int. J. Heat Mass Transfer* **108**, 417 (2017).
- <sup>96</sup>M. Prutton, *Acta Crystallogr., Sect. A: Found. Adv.* **31**, 526–527 (1975).
- <sup>97</sup>G. Kresse and J. Furthmüller, *Comput. Mater. Sci.* **6**, 15 (1996).
- <sup>98</sup>G. Kresse and J. Furthmüller, *Phys. Rev. B* **54**, 011169 (1996).
- <sup>99</sup>P. Geerlings, F. De Proft, and W. Langenaeker, *Chem. Rev.* **103**, 1793 (2003).
- <sup>100</sup>K. Burke, *J. Chem. Phys.* **136**, 150901 (2012).
- <sup>101</sup>W. Koch and M. C. Holthausen, *A Chemist's Guide to Density Functional Theory* (John Wiley & Sons, 2015).
- <sup>102</sup>L. Chaput, J. Larroque, P. Dollfus, J. Saint-Martin, and D. Lacroix, *Appl. Phys. Lett.* **112**, 033104 (2018).
- <sup>103</sup>J. M. Ziman, *Electrons and Phonons: The Theory of Transport Phenomena in Solids* (Oxford University Press, 2001).
- <sup>104</sup>G. P. Srivastava, *The Physics of Phonons* (Routledge, 2019).
- <sup>105</sup>A. Ward, D. A. Broido, D. A. Stewart, and G. Deinzer, *Phys. Rev. B* **80**, 125203 (2009).
- <sup>106</sup>S. Baroni, S. de Gironcoli, and P. Giannozzi, *Phys. Rev. Lett.* **65**, 84 (1990).
- <sup>107</sup>N. Marzari, S. De Gironcoli, and S. Baroni, *Phys. Rev. Lett.* **72**, 4001 (1994).
- <sup>108</sup>P. E. Hopkins, C. M. Reinke, M. F. Su, R. H. Olsson, E. A. Shaner, Z. C. Leseman, J. R. Serrano, L. M. Phinney, and I. El-Kady, *Nano Lett.* **11**, 107 (2011).
- <sup>109</sup>J.-K. Yu, S. Mitrovic, D. Tham, J. Varghese, and J. R. Heath, *Nat. Nanotechnol.* **5**, 718 (2010).
- <sup>110</sup>X. Li and R. Yang, *Phys. Rev. B* **86**, 054305 (2012).
- <sup>111</sup>M. Luisier, *Phys. Rev. B* **86**, 245407 (2012).
- <sup>112</sup>J. Dai and Z. Tian, *Phys. Rev. B* **101**, 041301 (2020).
- <sup>113</sup>S. G. Volz and G. Chen, *Phys. Rev. B* **61**, 2651 (2000).
- <sup>114</sup>S. Volz, J. B. Saulnier, G. Chen, and P. Beauchamp, *Microelectron. J.* **31**, 815 (2000).
- <sup>115</sup>J. Chen, G. Zhang, and B. Li, *Nano Lett.* **12**, 2826 (2012).
- <sup>116</sup>B. C. Daly, H. J. Maris, K. Imamura, and S. Tamura, *Phys. Rev. B* **66**, 024301 (2002).
- <sup>117</sup>K. Imamura, Y. Tanaka, N. Nishiguchi, S. Tamura, and H. J. Maris, *J. Phys.: Condens. Matter* **15**, 8679 (2003).
- <sup>118</sup>J. Chen, G. Zhang, and B. Li, *Appl. Phys. Lett.* **95**, 073117 (2009).
- <sup>119</sup>I. M. Felix and L. F. C. Pereira, *Sci. Rep.* **8**, 2737 (2018).
- <sup>120</sup>Y. Cheng, X. Wu, Z. Zhang, Y. Sun, Y. Zhao, Y. Zhang, and G. Zhang, *Nanoscale* **13**, 1425 (2021).
- <sup>121</sup>C. L. Mehta, *Il Nuovo Cimento* **28**, 401 (1963).
- <sup>122</sup>G. Chen, *J. Heat Transfer* **121**, 945 (1999).
- <sup>123</sup>X. Li and R. Yang, *J. Appl. Phys.* **113**, 104306 (2013).
- <sup>124</sup>B. Latour, S. Volz, and Y. Chalopin, *Phys. Rev. B* **90**, 014307 (2014).
- <sup>125</sup>J. A. Thomas, J. E. Turney, R. M. Iutzi, C. H. Amon, and A. J. McGaughey, *Phys. Rev. B* **81**, 081411(R) (2010).
- <sup>126</sup>J. M. Larkin, J. E. Turney, A. D. Massicotte, C. H. Amon, and A. J. H. McGaughey, *J. Comput. Theor. Nanosci.* **11**, 249 (2014).
- <sup>127</sup>K. Sääskilähti, J. Oksanen, J. Tulkki, and S. Volz, *Phys. Rev. B* **90**, 134312 (2014).

- <sup>128</sup>K. Sääskilähti, J. Oksanen, S. Volz, and J. Tulkki, *Phys. Rev. B* **91**, 115426 (2015).
- <sup>129</sup>A. A. Maradudin and A. E. Fein, *Phys. Rev.* **128**, 2589 (1962).
- <sup>130</sup>A. J. C. Ladd, B. Moran, and W. G. Hoover, *Phys. Rev. B* **34**, 5058 (1986).
- <sup>131</sup>Z. Zhang, Y. Guo, M. Bescond, J. Chen, M. Nomura, and S. Volz, *Phys. Rev. B* **103**, 184307 (2021).
- <sup>132</sup>Y. Wang, H. Huang, and X. Ruan, *Phys. Rev. B* **90**, 165406 (2014).
- <sup>133</sup>B. Latour and Y. Chalopin, *Phys. Rev. B* **95**, 214310 (2017).
- <sup>134</sup>Y. Liao, T. Shiga, M. Kashiwagi, and J. Shiomi, *Phys. Rev. B* **98**, 134307 (2018).
- <sup>135</sup>S. Datta, *Quantum Transport: Atom to Transistor* (Cambridge University Press, 2005), Vol. 9780521631457, pp. 1–404.
- <sup>136</sup>P. W. Anderson, *Phys. Rev.* **109**, 1492 (1958).
- <sup>137</sup>Y. Guo, M. Bescond, Z. Zhang, S. Xiong, K. Hirakawa, M. Nomura, and S. Volz, “Thermal conductivity minimum of graded superlattices due to phonon localization,” [arXiv:2105.01832](https://arxiv.org/abs/2105.01832) [cond-mat.mes-hall] (2021).
- <sup>138</sup>J. Chen, G. Zhang, and B. Li, *J. Chem. Phys.* **135**, 104508 (2011).
- <sup>139</sup>H. Honarvar, L. Yang, and M. I. Hussein, *Appl. Phys. Lett.* **108**, 263101 (2016).
- <sup>140</sup>D. Ma, H. Ding, H. Meng, L. Feng, Y. Wu, J. Shiomi, and N. Yang, *Phys. Rev. B* **94**, 165434 (2016).
- <sup>141</sup>S. Pailhès, H. Euchner, V. M. Giordano, R. Debord, A. Assy, S. Gomès, A. Bosak, D. Machon, S. Paschen, and M. De Boissieu, *Phys. Rev. Lett.* **113**, 025506 (2014).
- <sup>142</sup>Q. Xi, Z. Zhang, T. Nakayama, J. Chen, J. Zhou, and B. Li, *Phys. Rev. B* **97**, 224308 (2018).
- <sup>143</sup>C. Chen, Z. Zhang, and J. Chen, *Front. Energy Res.* **6**, 34 (2018).
- <sup>144</sup>D. Ma, X. Wan, and N. Yang, *Phys. Rev. B* **98**, 245420 (2018).
- <sup>145</sup>Z. Zhang, Y. Ouyang, J. Chen, and S. Volz, *Chin. Phys. B* **29**, 124402 (2020).
- <sup>146</sup>Z. Zhang, S. Hu, Q. Xi, T. Nakayama, S. Volz, J. Chen, and B. Li, *Phys. Rev. B* **101**, 081402(R) (2020).
- <sup>147</sup>H. Han, L. Feng, S. Xiong, T. Shiga, J. Shiomi, S. Volz, and Y. A. Kosevich, *Low Temp. Phys.* **42**, 711 (2016).
- <sup>148</sup>P. Jiang, Y. Ouyang, W. Ren, C. Yu, J. He, and J. Chen, *APL Mater.* **9**, 040703 (2021).
- <sup>149</sup>M. I. Hussein, C. N. Tsai, and H. Honarvar, *Adv. Funct. Mater.* **30**, 1906718 (2020).
- <sup>150</sup>T. Tadano, Y. Gohda, and S. Tsuneyuki, *Phys. Rev. Lett.* **114**, 095501 (2015).
- <sup>151</sup>Z. Zhang, S. Hu, T. Nakayama, J. Chen, and B. Li, *Carbon* **139**, 289 (2018).
- <sup>152</sup>H. Wang, Y. Cheng, M. Nomura, S. Volz, D. Donadio, X. Zhang, and S. Xiong, *Phys. Rev. B* **103**, 085414 (2021).
- <sup>153</sup>Y. A. Kosevich, L. G. Potyomina, A. N. Darinskii, and I. A. Strelnikov, *Phys. Rev. B* **97**, 094117 (2018).
- <sup>154</sup>Y. A. Kosevich and I. A. Strelnikov, *AIP Conf. Proc.* **1936**, 020002 (2018).
- <sup>155</sup>H. Han, B. Li, S. Volz, and Y. A. Kosevich, *Phys. Rev. Lett.* **114**, 145501 (2015).
- <sup>156</sup>A. H. Aly, A. Nagaty, and Z. Khalifa, *Int. J. Mod. Phys. B* **31**, 1750147 (2017).
- <sup>157</sup>X. Mu, L. Wang, X. Yang, P. Zhang, A. C. To, and T. Luo, *Sci. Rep.* **5**, 16697 (2015).
- <sup>158</sup>S. C. Huberman, J. M. Larkin, A. J. H. McGaughey, and C. H. Amon, *Phys. Rev. B* **88**, 155311 (2013).
- <sup>159</sup>J. Carrete, W. Li, N. Mingo, S. Wang, and S. Curtarolo, *Phys. Rev. X* **4**, 011019 (2014).
- <sup>160</sup>M. Yamawaki, M. Ohnishi, S. Ju, and J. Shiomi, *Sci. Adv.* **4**, eaar4192 (2018).
- <sup>161</sup>M. Ohnishi and J. Shiomi, *APL Mater.* **7**, 013102 (2019).
- <sup>162</sup>X. Wan, W. Feng, Y. Wang, H. Wang, X. Zhang, C. Deng, and N. Yang, *Nano Lett.* **19**, 3387 (2019).
- <sup>163</sup>S. Ju, S. Shimizu, and J. Shiomi, *J. Appl. Phys.* **128**, 161102 (2020).
- <sup>164</sup>Y. Ouyang, Z. Zhang, C. Yu, J. He, G. Yan, and J. Chen, *Chin. Phys. Lett.* **37**, 126301 (2020).
- <sup>165</sup>J. Yan, H. Wei, H. Xie, X. Gu, and H. Bao, *ES Energy Environ.* **8**, 56–64 (2020).
- <sup>166</sup>S. Hu, S. Ju, C. Shao, J. Guo, B. Xu, M. Ohnishi, and J. Shiomi, *Mater. Today Phys.* **16**, 100324 (2021).
- <sup>167</sup>Y. Liu, R. Hu, Y. Wang, J. Ma, Z. Yang, and X. Luo, *Energy AI* **3**, 100046 (2021).
- <sup>168</sup>R. Li, E. Lee, and T. Luo, *Mater. Today Phys.* **12**, 100181 (2020).
- <sup>169</sup>J. Guo, S. Ju, and J. Shiomi, “Application of Bayesian optimization to thermal science,” in *Nanoscale Energy Transport* (IOP Publishing, 2020), pp. 5-1–5-17.
- <sup>170</sup>J. A. Acebrón, L. L. Bonilla, C. J. Pérez Vicente, F. Ritort, and R. Spigler, *Rev. Mod. Phys.* **77**, 137 (2005).
- <sup>171</sup>G. Heinrich, M. Ludwig, J. Qian, B. Kubala, and F. Marquardt, *Phys. Rev. Lett.* **107**, 043603 (2011).
- <sup>172</sup>Z. Zhang, Y. Guo, M. Bescond, J. Chen, M. Nomura, and S. Volz, “Self-synchronization of thermal phonons at equilibrium,” [arXiv:2005.06711](https://arxiv.org/abs/2005.06711) [cond-mat.mes-hall] (2020).
- <sup>173</sup>M. Simoncelli, N. Marzari, and F. Mauri, *Nat. Phys.* **15**, 809 (2019).
- <sup>174</sup>L. Isaeva, G. Barbalinardo, D. Donadio, and S. Baroni, *Nat. Commun.* **10**, 3853 (2019).
- <sup>175</sup>S. Mukhopadhyay, D. S. Parker, B. C. Sales, A. A. Puretzy, M. A. McGuire, and L. Lindsay, *Science* **360**, 1455 (2018).
- <sup>176</sup>A. Jain, *Phys. Rev. B* **102**, 201201(R) (2020).
- <sup>177</sup>R. Peierls, “On the kinetic theory of thermal conduction in crystals,” in *Selected Scientific Papers of Sir Rudolf Peierls* (World Scientific, 1997), Vol. 43, pp. 15–48.